



**BNL-81624-2008-CP**

**Development of covariance capabilities in EMPIRE code**

M. Herman<sup>1</sup>, M.T. Pigni<sup>1</sup>, P. Oblozinsky<sup>1</sup>, S.F. Mughabghab<sup>1</sup>, C.M. Mattoon<sup>1</sup>,  
R. Capote<sup>2</sup>, Young-Sik Cho<sup>3</sup>, A. Trkov<sup>4</sup>

<sup>1</sup> *National Nuclear Data Center, Brookhaven National Laboratory, Upton, NY 11973, USA*

<sup>2</sup> *Nuclear Data Section, IAEA, Vienna, Austria*

<sup>3</sup> *KAERI, Daejeon, S. Korea and*

<sup>4</sup> *Jozef Stefan Institute, Ljubljana, Slovenia*

*Presented at the Covariance Workshop  
Port Jefferson, New York,  
June 24-27, 2008*

National Nuclear Data Center  
Energy Sciences & Technology Department  
**Brookhaven National Laboratory**  
P.O. Box 5000  
Upton, NY 11973-5000  
[www.bnl.gov](http://www.bnl.gov)

Notice: This manuscript has been co-authored by employees of Brookhaven Science Associates, LLC under Contract No. DE-AC02-98CH10886 with the U.S. Department of Energy. The publisher by accepting the manuscript for publication acknowledges that the United States Government retains a non-exclusive, paid-up, irrevocable, world-wide license to publish or reproduce the published form of this manuscript, or allow others to do so, for United States Government purposes.

## **DISCLAIMER**

This report was prepared as an account of work sponsored by an agency of the United States Government. Neither the United States Government nor any agency thereof, nor any of their employees, nor any of their contractors, subcontractors, or their employees, makes any warranty, express or implied, or assumes any legal liability or responsibility for the accuracy, completeness, or any third party's use or the results of such use of any information, apparatus, product, or process disclosed, or represents that its use would not infringe privately owned rights. Reference herein to any specific commercial product, process, or service by trade name, trademark, manufacturer, or otherwise, does not necessarily constitute or imply its endorsement, recommendation, or favoring by the United States Government or any agency thereof or its contractors or subcontractors. The views and opinions of authors expressed herein do not necessarily state or reflect those of the United States Government or any agency thereof.

# Development of covariance capabilities in EMPIRE code

M. Herman<sup>1</sup>, M.T. Pigni<sup>1</sup>, P. Obložinský<sup>1</sup>, S.F. Mughabghab<sup>1</sup>, C.M. Mattoon<sup>1</sup>,  
R. Capote<sup>2</sup>, Young-Sik Cho<sup>3</sup>, A. Trkov<sup>4</sup>

<sup>1</sup> *National Nuclear Data Center, Brookhaven National Laboratory, Upton, NY 11973, USA*

<sup>2</sup> *Nuclear Data Section, IAEA, Vienna, Austria*

<sup>3</sup> *KAERI, Daejeon, S. Korea and*

<sup>4</sup> *Jozef Stefan Institute, Ljubljana, Slovenia*

(Dated: today)

The nuclear reaction code EMPIRE has been extended to provide evaluation capabilities for neutron cross section covariances in the thermal, resolved resonance, unresolved resonance and fast neutron regions. The Atlas of Neutron Resonances by Mughabghab is used as a primary source of information on uncertainties at low energies. Care is taken to ensure consistency among the resonance parameter uncertainties and those for thermal cross sections. The resulting resonance parameter covariances are formatted in the ENDF-6 File 32.

In the fast neutron range our methodology is based on model calculations with the code EMPIRE combined with experimental data through several available approaches. The model-based covariances can be obtained using deterministic (Kalman) or stochastic (Monte Carlo) propagation of model parameter uncertainties. We show that these two procedures yield comparable results. The Kalman filter and/or the generalized least square fitting procedures are employed to incorporate experimental information. We compare the two approaches analyzing results for the major reaction channels on <sup>89</sup>Y. We also discuss a long-standing issue of unreasonably low uncertainties and link it to the rigidity of the model.

## I. INTRODUCTION

In recent years there has been an increasing demand from nuclear research, industry, safety and regulatory bodies for best estimate predictions of system performance, such as the design and operational parameters of nuclear reactors, to be provided with their confidence bounds. Estimates of the accuracy of predictions of such integral quantities can be obtained through the propagation of uncertainties in microscopic evaluated neutron cross section data.

A methodology for evaluating cross section covariance data has therefore been developed within the EMPIRE code system. The methodology covers the thermal energy, resolved resonance, unresolved resonance and fast neutron regions and builds on the following major components:

- Nuclear reaction model code EMPIRE [1]
- Atlas of Neutron Resonances [2]
- Kalman filter code [3] and Monte Carlo sampling [4].

The EMPIRE code is a key element in a broader effort pursued by the NNDC in developing covariance capabilities. This effort, that started with covariances in the fast neutron region, currently covers also the resonance region and extends to covariance visualization [5] and processing [6].

EMPIRE provides a natural environment for implementing the covariance evaluation capabilities. It is built around a physics core designed for modeling low- to-intermediate-energy nuclear reactions. It incorporates an extensive set of nuclear reaction models able to describe all relevant reaction mechanisms, each of them conveniently coupled to the up-to-date library of input model parameters [7]. The code is also suitable for massive calculations, is easy to use, has readily available default input values for all parameters, and is applicable to a wide range of target nuclei and incident neutron energies from about 1 keV to 150 MeV. Results may be stored

in ENDF-6 format and subsequently plotted against experimental data for verification.

EMPIRE now includes a newly-developed resonance module that extends its covariance capability to the thermal and resonance ranges. The module utilizes the recently published Atlas of Neutron Resonances [2], a monumental work by S.F. Mughabghab containing the resonance parameters frequently adopted by many evaluations in major evaluated data libraries. The resonance module contains an electronic version of these resonance parameters along with modernized versions of the legacy codes used to develop and maintain the Atlas. In addition, the Atlas contains parameter uncertainties and the resonance module was extended to utilize this information for producing covariances in the thermal and epithermal regions.

The generation of covariances at the NNDC is based on the deterministic Kalman filter technique, which is used in the thermal and resonance range as well as in the fast neutron range. The IAEA developers, who work only in the fast region, opted for the stochastic Monte Carlo (MC) procedure to generate the model-prior, coupled to the generalized least-squares code GANDR [8] to include the experimental data. There are several fundamental and operational differences between the two methods. MC propagates uncertainties of model parameters by means of random sampling while deterministic propagation of uncertainties, using the first-order Taylor expansion, is used in the Kalman approach. Accordingly, higher-order effects are included in MC but not in Kalman. The two approaches currently also differ regarding treatment of experimental data; it is naturally included in Kalman whereas a generalized least squares code GANDR must be run with the MC generated model-based prior as input.

The paper is organized as follows. In Chapter II we describe covariance methodology. Then, in Chapter III we discuss the resonance region, followed by Chapter IV devoted to fast neutrons. In Chapter V we summarize our covariance evaluations.

Conclusions are given in Chapter VI.

## II. COVARIANCE METHODOLOGY IN EMPIRE

### A. EMPIRE-KALMAN approach

The Kalman filter technique is used both in the resonance and in the fast neutron region. It is based on minimum variance estimation and naturally combines covariances of model parameters, of experimental data and of cross sections. This universality is a major advantage of the method. KALMAN uses measurements along with their uncertainties to constrain covariances of the model parameters via the sensitivity matrix. Then, the final cross section covariances are calculated from the updated covariances for model parameters. This procedure consistently accounts for the experimental uncertainties and the uncertainties of the model parameters ensuring that the final cross section uncertainties are at least as good as the smaller of the two. We emphasize that under the term ‘reaction model’ we mean also the resonance region described by models such as the Multi-Level Breit-Wigner formalism.

The key ingredient of the method is the sensitivity matrix, which represents complex nuclear reaction calculations. If we denote the combination of nuclear reaction models as an operator  $\hat{M}$  that transforms the vector of model parameters  $\mathbf{p}$  into a vector of cross sections  $\sigma(\mathbf{p})$  for a specific reaction channel, then the sensitivity matrix  $\mathbf{S}$  can be interpreted as the linear term in the expansion of the operator  $\hat{M}$ ,

$$\begin{aligned}\hat{M}\mathbf{p} &= \sigma(\mathbf{p}) \\ \hat{M}(\mathbf{p} + \delta\mathbf{p}) &= \sigma(\mathbf{p}) + \mathbf{S}\delta\mathbf{p} + \dots\end{aligned}\quad (1)$$

We use ‘hat’ to stress that  $\hat{M}$  is the operator rather than a matrix. In practice, the elements  $s_{i,j}$  of the sensitivity matrix are calculated numerically as partial derivatives of the cross sections  $\sigma$  at the energy  $E_i$  with respect to the parameter  $p_j$ ,

$$s_{i,j} = \frac{\partial\sigma(E_i, \mathbf{p})}{\partial p_j}. \quad (2)$$

In case of covariance determination, the initial values of the parameters,  $\mathbf{p}_1$ , are already optimized, *i.e.*, when used in the model calculations they provide the evaluated cross sections. Their covariance matrix  $\mathbf{P}_1$  is assumed to be diagonal while the uncertainties of the parameters are estimated using systematics, independent measurements or educated guesses. The model-based covariance matrix (prior) for the cross sections,  $\mathbf{C}_1$ , can be obtained through a simple error propagation formula,

$$\mathbf{C}_1 = \mathbf{S}\mathbf{P}_1\mathbf{S}^T, \quad (3)$$

where superscript T indicates a transposed matrix.

The experimental data, if available, are included through a sequential update of the parameter vector  $\mathbf{p}$  and the related

covariance matrix  $\mathbf{P}$  as

$$\begin{aligned}\mathbf{p}_{n+1} &= \mathbf{p}_n + \mathbf{P}_n\mathbf{S}^T\mathbf{Q}_n(\sigma_n^{\text{exp}} - \sigma(\mathbf{p}_n)) \\ \mathbf{P}_{n+1} &= \mathbf{P}_n - \mathbf{P}_n\mathbf{S}^T\mathbf{Q}_n\mathbf{S}\mathbf{P}_n.\end{aligned}\quad (4)$$

Here,

$$\mathbf{Q}_n = (\mathbf{C}_n + \mathbf{C}_n^{\text{exp}})^{-1}, \quad (5)$$

$n$  denotes the  $n^{\text{th}}$  step in the evaluation process related to the sequential inclusion of the  $n^{\text{th}}$  experimental data set, vector  $\mathbf{p}_{n+1}$  contains the improved values of the parameters starting from the vector  $\mathbf{p}_n$ , and  $\mathbf{P}_{n+1}$  is the updated covariance matrix of the parameters  $\mathbf{p}_{n+1}$ . The  $\mathbf{C}_n^{\text{exp}}$  is the cross section covariance matrix for the  $n^{\text{th}}$  experiment. The updated (posterior) covariance matrix for the cross sections is obtained by replacing  $\mathbf{P}_1$  with  $\mathbf{P}_{n+1}$  in Eq. (3),

$$\mathbf{C}_{n+1} = \mathbf{S}\mathbf{P}_{n+1}\mathbf{S}^T. \quad (6)$$

The updating procedure described above is often called Bayesian, although Eqs. (4-6) can be derived without any reference to the Bayes theorem as shown in Ref. [9].

The experimental covariance matrix,  $\mathbf{C}_n^{\text{exp}}$ , is usually non-diagonal, due to the correlations among various energy points  $E_i$ . Assuming that systematic experimental uncertainties are fully correlated, the matrix elements are expressed through the statistical,  $\Delta^{\text{sta}}\sigma_n^{\text{exp}}$ , and systematic,  $\Delta^{\text{sys}}\sigma_n^{\text{exp}}$ , experimental uncertainties. This yields

$${}_nC_{i,i}^{\text{exp}} = (\Delta^{\text{sta}}\sigma_n^{\text{exp}}(E_i))^2 + (\Delta^{\text{sta}}\sigma_n^{\text{exp}}(E_i))^2 \quad (7)$$

and, for  $i \neq k$ ,

$${}_nC_{i,k}^{\text{exp}} = \Delta^{\text{sys}}\sigma_n^{\text{exp}}(E_i) \times \Delta^{\text{sys}}\sigma_n^{\text{exp}}(E_k). \quad (8)$$

An important technical issue, which has to be addressed in most of the covariance methods, is ensuring that the energy grid,  $E_i$ , for the model calculations and experimental data is the same to enable matrix operations in Eqs. (4-6). In the KALMAN code this is achieved by bi-spline interpolation of model cross sections and sensitivity matrices.

The above description can easily be generalized to account for correlations among different experiments. To this end one should construct a single vector containing all experimental points and the related covariance matrix, which now may contain blocks correlating different experiments. Only one update is needed in such a case but the covariance matrices are much bigger (in the current implementation of the Kalman filter the model-based covariance matrix is expanded to match the experimental one).

The quality and consistency of the evaluated cross sections can be assessed by scalar quantity

$$\chi^2 = \sum_n (\sigma_n^{\text{exp}} - \sigma(\mathbf{p}_{\text{fin}}))^T (\mathbf{C}_n^{\text{exp}})^{-1} (\sigma_n^{\text{exp}} - \sigma(\mathbf{p}_{\text{fin}})), \quad (9)$$

where  $\mathbf{p}_{\text{fin}}$  is the final set of model parameters. A value of  $\chi^2$  per degree of freedom exceeding unity indicates underestimation of the evaluated uncertainties. It is a fairly common

practice to multiply such uncertainties by a square root of  $\chi^2$  per degree of freedom to address this issue.

The evaluator may choose to perform a sequential update using experimental data for several/all reactions or just for a single one. In the former case, all considered reactions are correlated and unique set of parameters along with the related covariance matrix are produced. On the other hand, poor experimental data in one reaction channel can negatively influence predictions for other channels.

We note that EMPIRE-KALMAN system is a general and powerful tool for evaluation of nuclear reactions. In addition to covariance calculations it may also be used to adjust model parameters to reproduce experimental cross sections and other observables within the selected reaction models and initial uncertainties of model parameters. Therefore, the Kalman filter can be used throughout the whole evaluation procedure to ensure consistency between cross sections, model parameters, and related covariance matrices.

### B. EMPIRE-MC approach

The Monte-Carlo (MC) method is used in EMPIRE only in the fast neutron region. Its application to determination of covariances for the nuclear reaction observables is very transparent [4]. First, model input parameters that play a significant role in defining reaction observables of interest are identified. Then, the EMPIRE code is run a number of times with relevant input parameters being drawn randomly within the assumed limits around the central (optimal) values of the parameters. Typically, a flat distribution is used for drawing but there is also a provision for the Gaussian one. Each such calculation covers the desired incident energy range and produces full set of cross sections, spectra, angular distributions and other observables. Standard statistical methods are used to obtain covariances for the calculated quantities automatically including cross-reactions correlations. The same approach can also be used for estimating cross-correlations between any two quantities.

The MC calculations are conceptually straightforward and free of certain simplifying assumptions, *e.g.*, the assumption of a linear response of the observables to the variation of parameters, which is inherent in the KALMAN method. There is no need for a preliminary sensitivity calculation and the computing time is independent of the employed number of model parameters. These advantages come at a price - the number of required calculations is in the range of hundreds and the convergence of the results has to be demonstrated.

The standard implementation of the MC method has no provision for incorporating experimental data; the uncertainties and correlations depend only on the assumed uncertainties of the model parameters. However, the so-obtained covariance matrix can be used as a prior in a full analysis by the generalized least-squares method, taking experimental data and their uncertainties rigorously into account, *e.g.*, the GANDR system had been used in recent IAEA evaluations. Furthermore, the model-based covariances obtained with the MC method constitute a reliable benchmark for validating the faster but

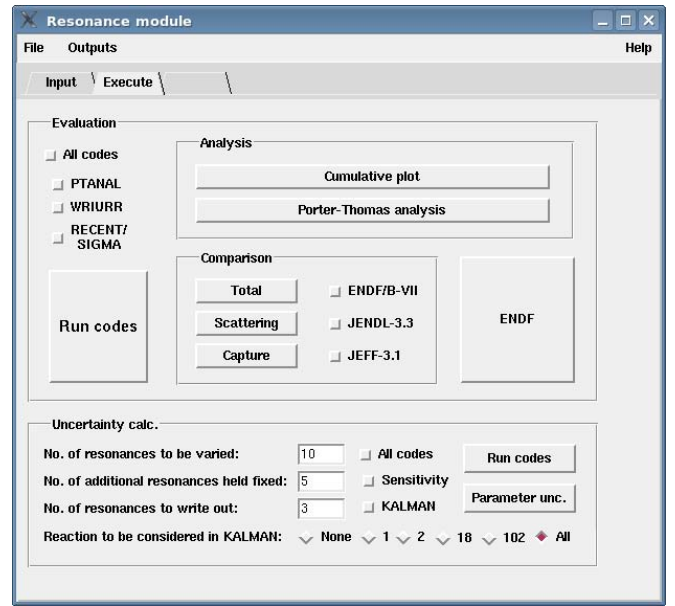


FIG. 1: Graphic user interface (GUI) of the EMPIRE resonance module. The buttons for covariance calculations are in the lower part.

linear-model calculations with KALMAN code.

## III. RESONANCE REGION

### A. EMPIRE resonance module

A new module for evaluating neutron cross sections in the resonance region automates most of the evaluation procedures and can be executed within EMPIRE or as a stand-alone program. It includes a graphic user interface (see Fig. 1) and a number of codes and scripts that read individual, as well as average, resonance parameters from the Atlas of Neutron Resonances [2] and other physical constants from RIPL-2 [7]. This allows performing a statistical analysis of the available resonances and computing cross sections in the resolved and unresolved resonance regions which are then compared with experimental data. The module also provides an ENDF-6 formatted file for a resonance region and various plots for verifying the procedure.

The PTANAL and WRIURR codes [10] constitute the computational core of the module. PTANAL assigns missing angular momentum and spin values to resonances using the Bayesian method and a random assignment method, respectively. It also assigns the mean radiative width to resonances with unknown  $\Gamma_\gamma$ . In addition, the reduced resonance widths are analyzed and fit with the Porter-Thomas distribution. The WRIURR code, starting from the Atlas values, constructs energy dependent average resonance parameters for the unresolved region and stores them in ENDF-6 format. All these tasks are executed with simple mouse clicks.

The reader is referred to Ref. [2] for more detailed explanation of the physics and mathematical formalism involved. The

fundamental roles of this new module are to preserve know-how accumulated over several decades by S. Mughabghab and to make it available in a modern computer environment. This will allow us to continue with the maintenance of the Atlas of Neutron Resonances in future.

### B. EMPIRE resonance covariance module

Initially, we took advantage of the fact that resonances are well described by a model such as Multilevel-Breit-Wigner (MLBW) with parameters fully deduced from experiments. Considering that often also their uncertainties were known, we extended the approach already developed for the fast region that was based on the propagation of parameter uncertainties into MF33 cross section uncertainties and correlations. This approach was used for producing covariances for  $^{89}\text{Y}$ ,  $^{99}\text{Tc}$  and  $^{191,193}\text{Ir}$  included in ENDF/B-VII.0 [11].

More recently, we realized that more straightforward approach would be to utilize MF32 representation of resonance parameter covariances and leave production of cross section covariances to the processing codes such as NJOY-99 and PUFF-IV. An initial study along these lines is available [12].

Following the above idea the resonance module has been extended to permit generation of MF32 covariances (see lower part of the Fig. 1). This is achieved in several steps:

- Uncertainties for resonance parameters and thermal values are retrieved from the electronic version of the Atlas. The missing information is supplied by making use of systematics or estimates. These uncertainties are put into an MF=32 file of resonance parameter covariances in the compact representation. This initial matrix is diagonal since no correlations are provided in the Atlas.
- The correlations between various parameters are estimated. In general, these are correlations for the same resonance, discussed in more detail by Mughabghab [13].
- The resonance parameter uncertainties are adjusted so that the uncertainties of thermal values are reproduced, as discussed below.

The resonance module has been designed to ensure consistency among thermal cross section uncertainties and uncertainties of the resonance parameters, a feature that was not addressed during the development of the Atlas database. Thermal cross sections are usually measured with higher accuracy than resonance parameters. In order to take advantage of their superior precision while still ensuring internal consistency of the estimated covariances, we have coupled the resonance module with the Kalman filter code, which allows for an objective adjustment of the original uncertainties. We illustrate such adjustment on the two extreme cases of neutron capture on  $^{55}\text{Mn}$  and  $^{90}\text{Zr}$ . In the case of  $^{55}\text{Mn}$  the thermal capture cross section is known with the accuracy of 0.37%, which is far better than the precision of the resonance parameters.  $^{90}\text{Zr}$  is a rare exception, in which the uncertainties in

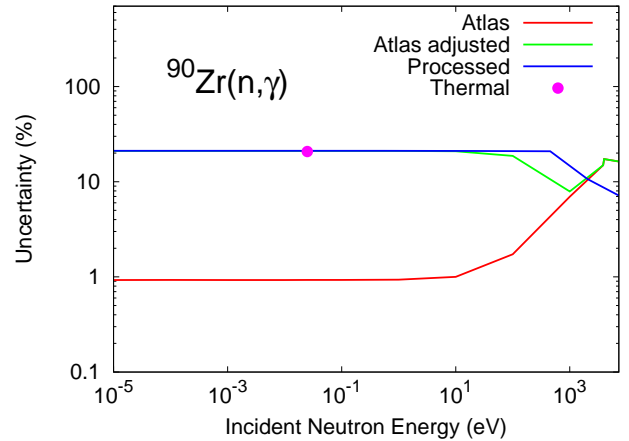


FIG. 2: Uncertainties of  $^{90}\text{Zr}(n, \gamma)$  cross sections. Compared is the direct propagation of the uncertainties of the resonance parameters reported in the Atlas (red), adjustment in which non-zero uncertainties were assigned to widths of the bound resonance (green) and the group-wise representation obtained with PUFF-IV (blue). The recommended uncertainty of the thermal value is also shown.

the resonance region are about three times smaller than for the thermal capture (20%).

The case of  $^{90}\text{Zr}$  is relatively straightforward - since propagation of the uncertainties of positive resonances to the thermal region falls short of the experimental capture uncertainty (see Fig. 2), we impose uncertainties of the neutron and radiative widths of the bound resonance. The original Atlas uncertainties of the positive resonances are preserved and there is no need for any correlations among parameters. The resulting uncertainties shown in Fig. 2 are in point-wise form. The same data in group form were taken from the contribution by Arcilla *et al.* [6]. The agreement is perfect in the thermal region, in which the cross sections are strongly correlated. In the region of resolved resonances the point-wise data are higher than the group uncertainties due to statistical averaging over uncorrelated resonances.

To address an inconsistency observed in the case of  $^{55}\text{Mn}$  we considered three scenarios:

1. Adjustment of the resonance parameter uncertainties without invoking correlations among the parameters.
2. Adjustment of the positive-energy resonances using Kalman filter technique, which implies considering a full covariance matrix of the parameters.
3. The same as in point 2 but including also bound (negative-energy) resonances in the analysis.

Detailed discussion of the first scenario, along with its application to the neutron radiative capture on  $^{55}\text{Mn}$ , was done by Mughabghab and Obložinský [13]. Restricting adjustment to the parameter uncertainties led to a considerable modification of the Atlas data.

In the second scenario we extend the above analysis by allowing correlations among resonance parameters, but restrict

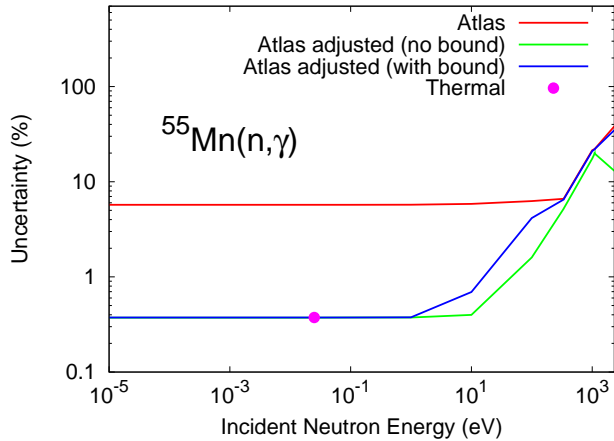


FIG. 3: Uncertainties of  $^{55}\text{Mn}(n, \gamma)$  cross sections. Direct propagation of the uncertainties of the resonance parameters reported in the Atlas (red) is compared with the results of the adjustment procedure with bound resonances excluded (green) and included (blue) in the analysis. The recommended uncertainty of the thermal value is also shown.

the analysis to the positive resonances. Fig. 3 shows that the adjustment brings uncertainties at the thermal energy into a perfect agreement with the experimental uncertainty. Inspection of the adjusted uncertainties in Table I (A1 column) indicates very small changes compared to the initial uncertainties (Atlas column). Only the radiative width uncertainty for the third resonance was changed significantly, by a factor of 0.3. The reduction of the capture cross section uncertainty at the thermal energy was obtained by introducing strong anti-correlations between the radiative widths of the three considered resonances.

The third scenario brings bound resonance(s) into the play, and treats them on the same footing as the positive-energy resonances. The generous initial uncertainties of the parameters for the two bound resonances (50% for the widths and 5% for the energies) are assumed to redirect the Kalman filter emphasis from the real resonances to the bound ones. Actually, the first bound and the first positive resonances are the major players contributing 27% and 59% of the thermal capture cross section, respectively. The results are plotted in Fig. 3, while the respective relative resonance parameters and their uncertainties are listed in columns A2 of Table I.

As in the second scenario, the Kalman filter makes use of the additional degrees of freedom and ensures low uncertainty in the thermal region by introducing anti-correlation among widths of bound resonances and widths of positive resonances, while correlations between radiative widths for the positive resonances are negligible. This treatment is consistent with the actual motivation for invoking negative resonances.

Fig. 4 shows the cross section correlation matrix obtained within this approach. The thermal region appears to be fully correlated, while the resolved resonances tend to be uncorrelated. Apart from the transitional region around 10 eV there are no correlations between the thermal and resolved reso-

TABLE I: Relative values and uncertainties of  $^{55}\text{Mn}$  resonance parameters for the two bound and the first three positive-energy resonances. A1 refers to values obtained when only the first three positive resonances were allowed to be varied, while A2 values were obtained when also the two bound resonances were included in the adjustment. The uncertainties of Ref. [2] are labeled as Atlas. The negative resonance numbers indicate bound resonances,  $E_0$  stands for the resonance energy,  $\Gamma_n$  and  $\Gamma_\gamma$  for the neutron and radiative width, respectively.

Res. #		Relative Value		Uncertainty (%)		
		A1	A2	Atlas	A1	A2
-2	$E_0$	1.000	1.000	0.00	0.00	4.99
	$\Gamma_n$	1.000	1.031	0.00	0.00	48.71
	$\Gamma_\gamma$	1.000	1.030	0.00	0.00	48.41
-1	$E_0$	1.000	1.007	0.00	0.00	4.87
	$\Gamma_n$	1.000	1.317	0.00	0.00	28.29
	$\Gamma_\gamma$	1.000	1.317	0.00	0.00	28.29
1	$E_0$	.999	.999	.30	.30	.30
	$\Gamma_n$	1.015	1.001	2.19	2.11	2.18
	$\Gamma_\gamma$	1.130	1.009	6.45	4.64	6.31
2	$E_0$	.999	1.000	.18	.18	.18
	$\Gamma_n$	1.004	1.000	4.44	4.42	4.44
	$\Gamma_\gamma$	1.119	1.008	22.98	20.31	22.77
3	$E_0$	.999	.999	.22	.22	.22
	$\Gamma_n$	1.018	1.001	5.22	5.09	5.21
	$\Gamma_\gamma$	2.011	1.075	38.24	12.36	34.77

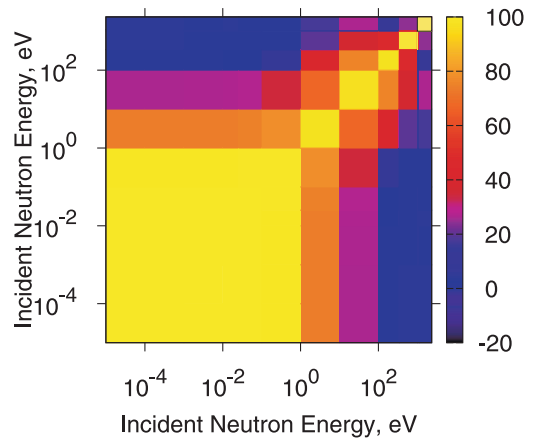


FIG. 4: Cross section correlations for  $^{55}\text{Mn}(n, \gamma)$  in the low energy region for the full adjustment scenario (A2, Table I). The thermal region (bottom-left, in yellow) is fully correlated.

nance regions.

In spite of limited experience with the adjustment, we tend to favor the latter scenario. It achieves the consistency of uncertainties while minimizing changes to the original Atlas values and avoiding anti-correlations between positive resonances.

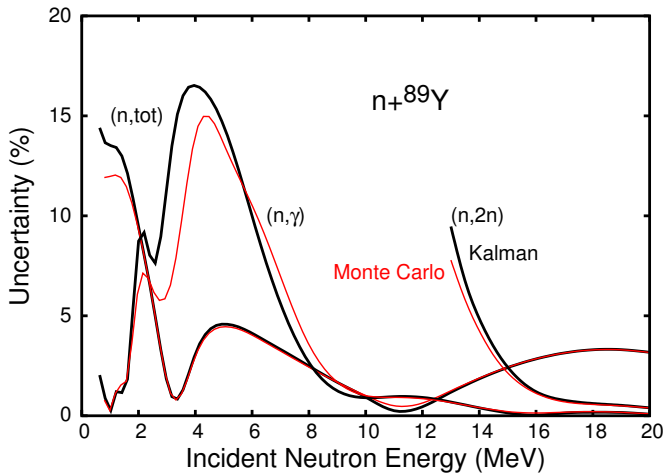


FIG. 5: Comparison of the model-based cross section uncertainties obtained with KALMAN (black) and Monte Carlo (red) methods for  $^{89}\text{Y}+n$  reactions. Calculated uncertainties result from the variation of the real depth of the optical potential.

#### IV. FAST NEUTRON REGION

##### A. Comparison of model-based covariances obtained with Monte Carlo and KALMAN

It is of fundamental importance to compare KALMAN and MC approaches and understand any differences. The EMPIRE code was employed to perform nuclear reaction calculations, which enter both approaches, keeping inputs in both methods identical. Thus, the potential source of discrepancies, inevitable if two different reaction codes were used, was avoided. Calculations were performed for total, elastic, inelastic,  $(n,2n)$ , capture,  $(n,p)$  and  $(n,\alpha)$  reactions on  $^{89}\text{Y}$  up to an incident energy of 20 MeV. The same uncertainties of model parameters were assumed and the MC parameters were sampled from a Gaussian distribution.

We have compared uncertainties of the considered cross sections resulting from the variation of a single model parameter. Fig. 5 shows such a comparison for one of the key parameters - depth of the real part of the optical potential. There is a reasonable agreement between model-based uncertainties obtained using the MC and KALMAN methods. Also, for the remaining parameters the results are close to each other. The only exception is the preequilibrium strength, for which the non-negligible differences were obtained. The reason for this discrepancy might be related to the fact that the relatively strong variation (20%) used in the calculations, together with the Gaussian distribution, allowed for values considerably far from the central value in the MC simulations. Because of this, the MC results may be demonstrating sensitivity to the non-linear dependence of the cross sections on the parameters.

Fig. 6 compares correlation matrices for the total cross sections. Again, both methods yield essentially equivalent results - the chess-board like pattern in the correlation matrix is the same in both methods. Only the transition between negative and positive correlations above 10 MeV is more gradual in the

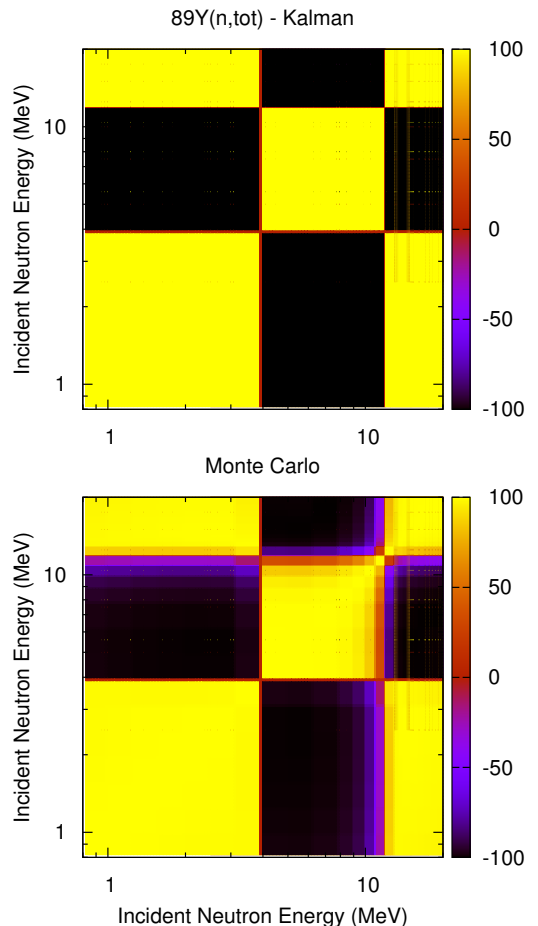


FIG. 6: Comparison of the model-based cross section correlations for  $^{89}\text{Y}(n,\text{tot})$  obtained with KALMAN (top) and Monte Carlo (bottom) methods. The correlations result from the variations of the real depth of the optical potential.

MC than in the KALMAN approach.

These numerical tests indicate that, in absence of experimental data, both methods are practically equivalent as long as the non-linearity (higher-order) effects in the KALMAN approach are taken into account. We found that to minimize the impact of non-linearity, the sensitivity matrix should be calculated using model parameter variations that are close to the parameter uncertainties.

##### B. Inclusion of experimental data

Inclusion of experimental data into the covariance determination still appears to be a major issue. The KALMAN method accounts for them naturally but suffers from the general deficiency of all least squares type approaches - uncertainties tend to reach values that are considered far too small if very many experimental data are included in the analysis. One practical remedy to this problem is to prevent uncertainties of the model parameters to fall below some sensible limit (say 3%). While this procedure is simple and effective, it in-

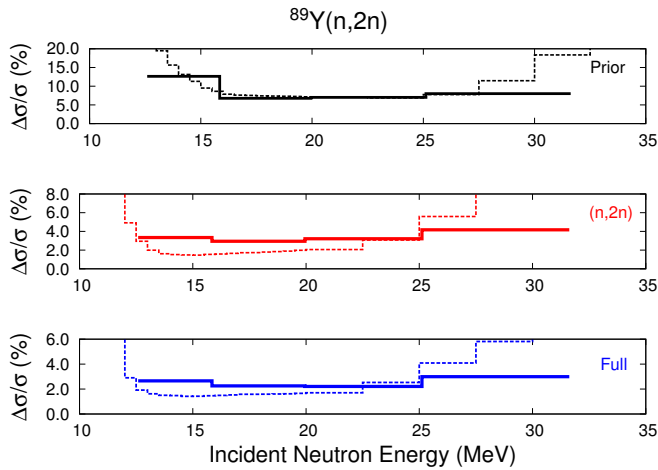


FIG. 7: Comparison of the  $^{89}\text{Y}(n,2n)$  cross section uncertainties obtained with GANDR (solid lines) and KALMAN (dashed lines) illustrating inclusion of experimental data. The top panel shows the model-based uncertainties (prior), the middle panel includes (n,2n) data only, and the bottom panel includes experimental data for all reaction channels.

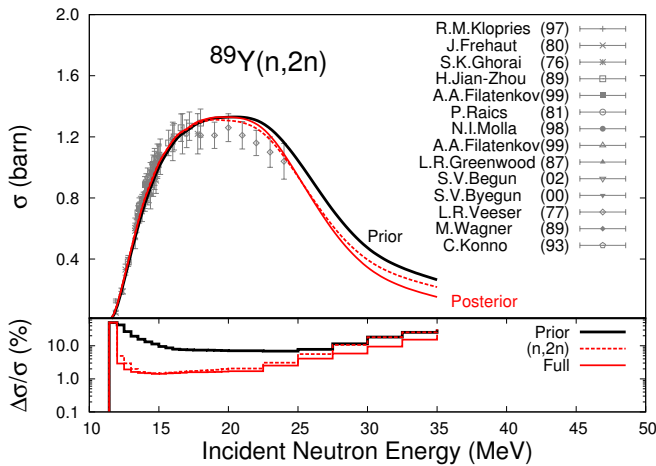


FIG. 8: Comparison of the  $^{89}\text{Y}(n,2n)$  cross sections and uncertainties obtained with KALMAN. ‘Prior’ indicates default calculations and related model-based uncertainties, ‘(n,2n)’ takes into account (n,2n) experimental data, and ‘Full’ includes experimental data for all reaction channels.

roduces a highly arbitrary component into the estimation of uncertainties. In the present comparison we have refrained from resorting to this solution.

The classical formulation of the MC approach does not account for the experimental data. Thus, in the present study, the prior (model-based cross section covariance), obtained with the EMPIRE-MC calculations, was fed into the Generalized Least Squares code ZOTT incorporated in a more general GANDR system by D.W. Muir [8]. In the following we refer to this approach as EMPIRE-MC-GANDR. The same nuclear reaction input was used to produce sensitivity matrices for KALMAN and the MC based priors for GANDR.

Fig. 7 illustrates effect of including experimental uncertain-

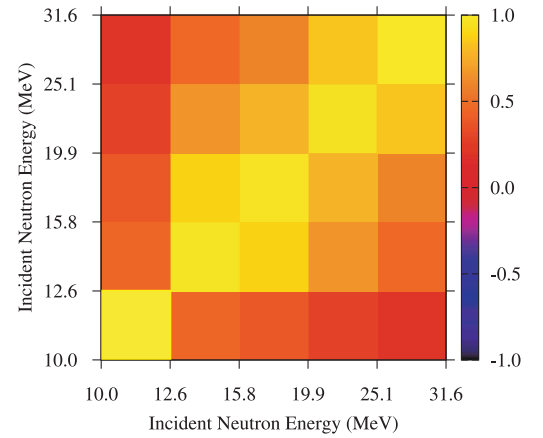
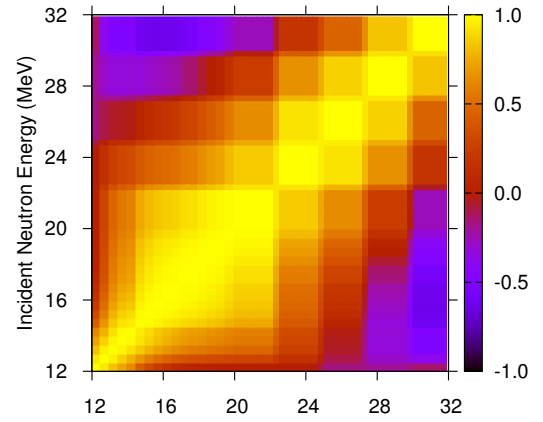


FIG. 9: The correlation matrix for the  $^{89}\text{Y}(n,2n)$  reaction obtained with KALMAN using full set of experimental data for all reaction channels (top). The same for MC method (bottom).

ties of the  $^{89}\text{Y}(n,2n)$  reaction estimated using the two methods. The pure model-based predictions are very similar. As expected, adding experimental data reduces uncertainties in both methods, but the reduction in the KALMAN approach is stronger than in the GANDR method. Inclusion of the experimental data for all the remaining channels (including nearly 1000 points for total) reduces (n,2n) uncertainties by about 30% in GANDR. In KALMAN this difference is practically negligible around 14-15 MeV, *i.e.*, in the range in which many (n,2n) measurements are available as can be seen in Fig. 8. This figure shows also the effect of including all experimental data on the posterior cross sections. Additional experimental points constrain model parameters so that the fit is slightly worse than in the case of using (n,2n) data only. There is a considerable advantage in reproducing all reaction channels simultaneously with the same set of model parameters, as cross correlations among various reaction channels are also produced.

Fig. 9 presents correlation matrices obtained with the two methods. The comparison is to some extent obscured by the low energy resolution in the case of GANDR, but the general structure of the two matrices can be considered similar. In the KALMAN matrix one notes relatively weak correlations

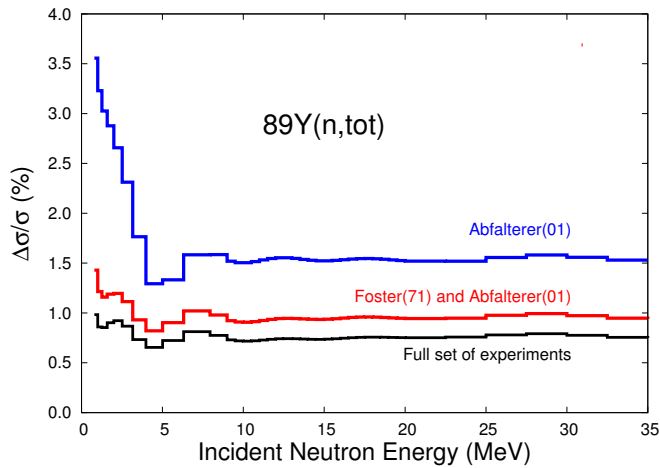


FIG. 10: Uncertainties of  $^{89}\text{Y}(n,\text{tot})$  cross sections obtained with KALMAN including (n,tot) data by Abfalterer (blue), (n,tot) data by Foster and Abfalterer (red), and full set of experimental data for all reaction channels (black).

below 15 MeV due to a large number of experimental data available in this region. At higher energies, the correlations are stronger as expected for the model dominated cases. The anticorrelations observed above 28 MeV can be explained as due to the preequilibrium emission that decreases (n,2n) cross sections in the maximum of the excitation function and increases them in the high energy tail.

Finally, in Fig. 10 we show  $^{93}\text{Nb}(n,\text{tot})$  and illustrate effect of including experimental data on the uncertainties of the total cross section using the KALMAN method. We note that 2.8% systematic error was assumed for all experiments but no cross correlations were allowed. Using the extended set of Abfalterer data (more than 400 points) the uncertainties are of the order of 1.5%. Adding about 200 points by Foster brings them down to about 1%, and including the remaining experiments results in a further reduction to about 0.75%. Many experimentalists would consider such low uncertainties as unrealistic.

### C. Avoiding unreasonably low uncertainties

Quite often, Kalman filter analysis involving a vast amount of experimental data results in uncertainties that are far lower than systematic uncertainties even of the most precise measurement. This happens in spite of the fact that proper experimental covariances, accounting for systematic uncertainties, are supplied as an input to the KALMAN code.

One of the sources of the problem is the implicit Kalman filter assumption that the model itself is perfect. Thus, any uncertainties in model calculations are only due to the uncertainties of the model parameters. Often, the shape of a calculated excitation function is constrained. We illustrate this point on the example of the  $^{93}\text{Nb}(n,\text{tot})$  reaction in Fig. 11. The depth and radius of the real part of the optical model potential are essentially determining the shape and magnitude of

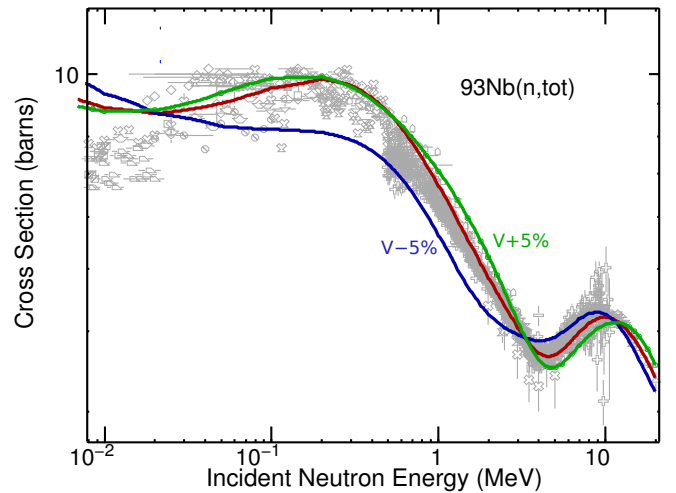


FIG. 11: Effect of 5% variation of the depth of the real optical potential on the  $^{93}\text{Nb}(n,\text{tot})$  cross section. The baseline values are in red.

the total cross section. The two quantities are known to be strongly correlated, therefore it is sufficient to consider only one of them. In Fig. 11 we show the change of total cross section in response to the variation of the real potential depth by 5%. One observes that this does not provide for scaling of the absolute value of the cross section. Such scaling is actually the degree of freedom that would be needed to accommodate systematic uncertainties in the measurements that in most cases amount to scaling cross sections up and down without changing its shape. Lack of this possibility might have a dramatic effect on parameter uncertainties - any scaling of the cross section appears incompatible with the model calculations since it can not be reproduced by any sensible variation of the model parameters. If the model were perfect we would have to conclude that the systematic experimental uncertainties are overestimated. To avoid such a reduction we introduce intrinsic model uncertainty by defining a fictitious model parameter,  $p_{\text{mod}}$ , that multiplies model predicted cross sections. The prior value of this parameter is one.

Our preliminary studies indicate that the Kalman filter adjusts the uncertainty of the fictitious model parameter,  $\Delta p_{\text{mod}}$ , to reproduce the smallest systematic uncertainty. Thus, if the whole energy range is adequately covered by the experimental data the final result is well-defined. In the energy ranges without measurements the result, to some extent, depends on the initial (assumed) uncertainty of the new parameter,  $\Delta p_{\text{mod}}$ . Naturally, if no experimental data are available the discussed contribution to the uncertainty is defined by  $\Delta p_{\text{mod}}$ . In such a case, however, the cross section uncertainties are determined primarily by the propagation of uncertainties of the genuine model parameters, which are much larger than the intrinsic model uncertainties. The latter can, therefore, be neglected especially since there should be no uncertainties small enough to raise any concern. The procedure is particularly useful to simulate intrinsic uncertainties in the optical model, *i.e.*, it is meant to be applied to the total cross sections. These are often very well measured which, combined with the rigid shape of

the optical model predictions, results in extremely low uncertainties. There is no need to invoke such a procedure for other nuclear reaction models, e.g., compound nucleus and preequilibrium emission, since their formulations include parameters which, to a large extent, provide for a scaling degree of freedom.

A conceptually similar solution, correlated sampling of energy-dependent scaling parameters, has also been adopted for the MC approach in EMPIRE. In this way, the minimum uncertainty of the calculated cross-section is limited by the uncertainty of the scaling parameter which is taken as the model uncertainty.

An additional source of low uncertainties has been discussed in the contribution by Leeb [14] to the present Workshop - neglecting correlations among numerous experiments implies statistical independence of the respective systematic uncertainties and leads to reducing final uncertainty below individual systematic uncertainty. We refer to the original paper by Leeb for a description of an approximate method allowing one to avoid this source of underestimation.

## V. APPLICATION TO COVARIANCE EVALUATIONS

The EMPIRE-KALMAN and EMPIRE-MC-GANDR system has been extensively applied for the generation of covariance data. We mention here covariances for 13 materials,  $^{89}\text{Y}$ ,  $^{99}\text{Tc}$ ,  $^{152-158,160}\text{Gd}$ ,  $^{191,193}\text{Ir}$  and  $^{232}\text{Th}$ , included in the new ENDF/B-VII.0 library [11] released in 2006. In addition, there was a considerable effort to deliver preliminary covariances for the WPEC Subgroup 26 which resulted in covariance estimates for 36 materials. The more recent large-scale project was initiated by the U.S. Nuclear Criticality Safety Program to provide a ‘low-fidelity’, but complete, set of covariances that could be used to exercise processing methodologies and tools [15].

New evaluations for a full set of stable tungsten isotopes,  $^{180,182-184,186}\text{W}$ , in the neutron energy range up to 150 MeV were produced [16], with the covariance matrices generated using the EMPIRE-MC-GANDR approach. The NNDC produced new covariances for  $^{55}\text{Mn}$  and  $^{90}\text{Zr}$  in the fast neutron region using EMPIRE-KALMAN technique [17].

The NNDC and LANL are cooperating in preparation of covariances for the ENDF/B-VII.0 data adjustment within the GNEP project. This activity involves about 100 materials relevant to the design of the innovative fast actinide burner reactors.

## VI. CONCLUSIONS

There has been considerable activity to reestablish covariance capabilities within the nuclear data community. Qualitative progress became possible due to the availability of advanced nuclear reaction codes supported by the comprehensive libraries of input parameters (RIPL) and by the compilation of resonance parameters (Atlas). The cross section covariance capabilities of the EMPIRE code cover the full energy range

relevant to applications, including thermal, resonance and fast neutron regions. This puts EMPIRE in a unique position to provide complete sets of covariance data for most of the nuclei, such as the fission products and structural materials. The code is also well capable of treating actinides. The modules for estimating covariances for neutron multiplicities and for fission spectra are integrated into the EMPIRE code but need adequate parametrization.

The resonance module of EMPIRE closes the gap between the evaluated neutron resonance data for 381 isotopes contained in the Atlas of Neutron Resonances and applications by bringing Atlas data into the evaluated nuclear data files. In particular, the module produces covariances of the resonance parameters in the MF32 compact representation. When doing this, the module allows adjustment of the parameter uncertainties in order to ensure consistency with the uncertainties of the thermal cross sections. We have discussed several strategies for imposing such consistency and found that in most cases invoking correlations among positive and negative (bound) resonances is the least intrusive solution.

In the fast neutron region we discussed two complementary methods implemented in EMPIRE for determining covariances. The Kalman filter approach is based on variance minimization while the stochastic one is based on the Monte Carlo sampling followed by the GANDR least-squares fitting of experimental data. We have compared both approaches and concluded that model-based covariances obtained with the two methods are practically equivalent. There is also a possibility of using KALMAN generated model-based prior with the GANDR code.

Very serious concerns were raised regarding extremely low uncertainties resulting from the least-squares analysis using model-generated priors. We believe that these low uncertainties arise, in part, from the rigidity of the model predictions, *i.e.*, intrinsic model uncertainties which are not accounted for in the procedure. Our numerical experiments indicate that adding new degrees of freedom to the model has a desired effect on the output uncertainties and might be used to eliminate this deficiency.

The EMPIRE code system is entering a stage at which it can effectively be used for production of covariance data. Still, there is a number of issues that should be addressed. In the resonance region these include accounting for the uncertainties of the resonance integrals, and possible correlations among positive resonance parameters. The methodology in the unresolved resonance region should be addressed by adding capability to utilize average resonance parameters. In the fast neutron range, we should be seeking better insight into intrinsic model uncertainties and expand the space of perturbed parameters, *e.g.*, we should include the energy dependence on the model parameters. Protracted activities along these lines should eventually provide an extensive and consistent set of model parameters. Last, but not least, is the long standing problem of analyzing experimental data in order to extract critical information regarding statistical and systematic errors associated with these measurements, which are decisive in determining evaluated data.

The work at BNL was sponsored by DOE-NNSA, DOE-NE, and also by DOE-Office of Science under Contract No.

DE-AC02-98CH10886 with Brookhaven Science Associates, LLC.

- 
- [1] M. Herman, R. Capote, B. Carlson, P. Obložinský, M. Sin, A. Trkov, H. Wienke, and V. Zerkin, "EMPIRE: Nuclear Reaction Model Code System for Data Evaluation," *Nuclear Data Sheets*, vol. **108**, no. 12, pp. 2655–2715, 2007.
- [2] S. F. Mughabghab, *Atlas of Neutron Resonances: Thermal Cross Sections and Resonance Parameters*. Amsterdam: Elsevier, 2006.
- [3] T. Kawano and K. Shibata, "Covariance Evaluation System." JAERI Data/Code, Japan Atomic Energy Research Institute, Tokai, Japan, 1997.
- [4] D. Smith, "Covariance matrices for nuclear cross sections derived from nuclear model calculations," report ANL/NDM-159 November, Argonne National Lab, 2004.
- [5] B. Pritychenko and A. Sonzogni, "Sigma: Web Retrieval Interface for Nuclear Reaction Data," *December 2008 issue of Nuclear Data Sheets*.
- [6] R. Arcilla, A. Kahler, P. Obložinský, and M. Herman, "Processing of Neutron Cross Section Covariances Using NJOY-99 and PUFF-IV," *December 2008 issue of Nuclear Data Sheets*.
- [7] T. Belgia, O. Bersillon, R. Capote, T. Fukahori, G. Zhigang, S. Goriely, M. Herman, A. Ignatyuk, S. Kailas, A. Koning, P. Obložinský, V. Plujko, and P. Young, "Handbook for Calculations of Nuclear Reaction Data, Reference Input Parameter Library-2," TECDOC-1506, IAEA, Vienna, 2005.
- [8] D. W. Muir, A. Mengoni, and I. Kodeli, "Integration International Standards Evaluation into a Global Data Assessment," *December 2008 issue of Nuclear Data Sheets*.
- [9] D. W. Muir, "Evaluation of correlated data using partitioned least squares: a minimum-variance derivation," *Nucl. Sci. Eng.*, vol. 101, pp. 88–93, 1989.
- [10] S. Oh, J. Chang, and S. F. Mughabghab, "Neutron cross section evaluations of fission products below the fast neutron region," Tech. Rep. BNL-NCS-67469, Brookhaven National Lab., 2000.
- [11] M. Chadwick, P. Obložinský, M. Herman, *et al.*, "ENDF/B-VII.0: Next generation evaluated nuclear data library for nuclear science and technology," *Nuclear Data Sheets*, vol. 107, no. 12, pp. 2931–3118, 2006.
- [12] M. Herman, S. Mughabghab, P. Obložinský, M. Pigni, and D. Rochman, "Neutron cross section covariances in the resolved resonance region," Report BNL-80173-2008, Brookhaven National Laboratory, 2008.
- [13] S. F. Mughabghab and P. Obložinský, "Neutron Cross Section Covariances in the Thermal and Resonance Regions," *December 2008 issue of Nuclear Data Sheets*.
- [14] H. Leeb, "Consistent procedure for evaluation based on modeling," *December 2008 issue of Nuclear Data Sheets*.
- [15] R. Little *et al.*, "Low-fidelity Covariance Project," *December 2008 issue of Nuclear Data Sheets*.
- [16] A. Trkov, R. Capote, I. Kodeli, and L. Leal, "Evaluation of Tungsten Nuclear Reaction Data with Covariances," *December 2008 issue of Nuclear Data Sheets*.
- [17] M. Pigni, M. Herman, and P. Obložinský, "Estimated  $^{55}\text{Mn}$  and  $^{90}\text{Zr}$  Covariances in the Fast Neutron Region," *December 2008 issue of Nuclear Data Sheets*.